International Journal of Electrical and Computer Engineering (IJECE)
Vol. 13, No. 4, August 2023, pp. 3733~3746
ISSN: 2088-8708, DOI: 10.11591/ijece.v13i4.pp3733-3746

DC-link voltage balancing and control of qZ-source inverter fed induction motor drive

Thin Zar[1], Mai Kai Suan Tial[2], Tun Lin Naing[1]
[1]Department of Electrical Power Engineering, Mandalay Technological University, Mandalay, Myanmar
[2]Department of Electrical Power Engineering, Yangon Technological University, Yangon, Myanmar

Article Info

Article history:

Received Mar 2, 2022
Revised Dec 27, 2022
Accepted Jan 19, 2023

Keywords:

Capacitor voltage-balancing
DC-link voltage control
Field-oriented control
qZ-source T-type inverter
Triple sixty-degree pulse width modulation

ABSTRACT

Poor performance of the motor drive system is caused when the direct current-link (DC-link) capacitor voltages of the inverter are not sufficiently generated. This is mainly because of the various load torque changes and input voltage fluctuation. The qZ-source inverter operates with a fully shoot-through technique. This technique causes mismatching between the upper and lower DC-link capacitor voltages. Without capacitor voltage-balancing function, the desired DC-link capacitor voltages could not be provided or maintained when there are load and speed changes. A Sawtooth carrier-based simple boost triple-sixty-degree (TSD) pulse width modulation (PWM) technique is used to drive the qZ-source T-type inverter because this technique can give a more significant boost DC-link voltage than a traditional simple boost PWM technique. Proportional integral (PI) controller is applied for the DC-link voltage controller to achieve the fast response and less steady-state error. The simulation model was constructed for a 4 kW, 400 V, 1,400 rpm induction motor (IM) drive system used in rolling mill using MATLAB/Simulink with and without voltage balancing function. As a result, DC-link voltages of the qZ-source T-type inverter fed the induction motor drive system could be controlled using a capacitor voltage-balancing function and the output power of the motor from the simulation result is approximately equal to 4 kW.

Corresponding Author:

Tun Lin Naing
Department of Electrical Power Engineering, Mandalay Technological University
Patheingyi, Mandalay, Myanmar
Email: tunlinnaing1980@gmail.com

1. INTRODUCTION

Traditional voltage source inverters (VSIs) are used in many applications of power electronic research area. Voltage source inverters are the buck inverter and cannot resist the shoot-through state which can damage the semiconductor devices. Therefore, VSIs need dead time to avoid the shoot-through condition. If dead time is used in VSI, the output voltage waveform distortion occurs in it. Impedance source (Z-source) voltage fed inverter was investigated in 2003 [1] to overcome the VSI's obstacle. The impedance network or impedance source interconnected between the direct current (DC) source and inverter can withstand the shoot-through state and does not damage the semiconductor devices. Moreover, it can get buck-boost features of the inverter output voltage by applying the shoot-through duty ratio. In this way, the impedance network placement in front of the inverter can achieve a more effective power conversion unit than using a DC-DC boost converter. Many researchers renovated the Z-source network improved its quality to get continuous input current during the working time. This new topology is called the quasi-impedance source (qZ-source) inverter. Besides, qZ-source inverter fed motor drive system can provide the ride-through capacitor voltage capability during input voltage sag, less harmonic, extend output voltage than voltage and current source inverter [2], [3]. The

improper values of inductors and capacitors called passive components used in the qZ-source inverter introduce the DC-link voltage spike and discontinuous mode condition. Therefore, it is necessary to select the proper values of passive components of the quasi network to achieve the effectiveness of the DC-link voltage [4]–[9].

In a three-level T-type inverter, there are upper and lower DC-link voltages which are separately controlled by the upper and lower shoot-through duty ratio, d_U and d_L. However, when the fully active state occurs, the upper and lower DC-link voltages are different. This is because the actual characteristics of passive components are different from that of data sheets. To ensure the desired upper and lower DC-link capacitor voltage, DC-link capacitor voltage-balancing function has been proposed [10]. A three-level T-type inverter fed induction motor drive system is efficient for medium switching frequency (4 to 24 kHz) and causes low conduction and switching losses and improve the efficiency of the drive system [11], [12]. According to the study [13], the T-type inverter is less blocking voltage and switching losses and improves efficiency of the drive system than other voltage source inverter. Moreover, the voltage-balancing condition of three-level T-type inverter topology with the proposed space vector (SV) pulsed width modulation (PWM) control strategy is better than the neutral point clamp (NPC) inverter [14].

Electric motor and generator are rotating machines used for the industrial applications such as integrated with advanced variable-frequency power converter, sensors, high performance variable-speed drives and control system. Such machines are designed to operate with three-phase and single-phase AC/DC voltage source. Generally, electric motors can be classified as DC, induction and synchronous motor. Among them, induction motor is rugged, reliable, low maintenance, less expensive, and widely used in industrial electric drives and automation drive system [15]. The control strategies implemented for drive systems are scalar control and vector control. The scalar or volt per hertz (V/f) control is simple and poor torque performance in the steady-state condition. The vector or field-oriented control (FOC) is a fast dynamic performance of speed and torque response at steady-state and transient conditions. Therefore, vector control becomes the most popular control technique in the induction motor (IM) drive system. In vector control, there are direct and indirect vector controls. By using direct vector control, the flux angle can be directly obtained from flux itself. However, the flux can be measured using the flux sensor in the air gap or sensing coil mounted on the induction motor. The flux sensor installation is complicated and expensive. Thus, it is not suitable for industrial applications. On the other hand, in indirect vector control, the flux angle can be obtained from the slip angular velocity estimated from the dq-axes current command for the required flux and torque produced. This method needed to separate the stator current into the flux producing component (d-axis stator current), and torque producing component (q-axis stator current) like as a separately excited DC motor [16], [17].

A qZ-source inverter fed induction motor drive system based indirect field-oriented control (IFOC) using in any dusty environment. In industrial application, voltage source inverter (VSI) fed vector control has been used to control the speed of the rolling mill by reducing the negative torque feedback [18]. The change in speed and load may cause the fluctuation in DC-link voltage of the inverter. However, there is no DC-link voltage control in this study while controlling the speed of the motor. Therefore, in this paper, the qZ-source T-type inverter fed vector control is developed to control the DC-link voltage for the motor drive system at changing speed and load. The T-type inverter with three main arms and three auxiliary arms is combined with qZ-source. In qZ-source T-type inverter, the upper and lower DC-link capacitor voltages are separately controlled. In this work, a new technique, a triple sixty-degree (TSD) PWM technique is used to control the upper and the lower capacitor voltage by applying the upper and lower duty ratio d_U and d_L. To balance the upper and lower DC-link voltages, a capacitor voltage-balancing function is used. Without this function, the over-boost will occur and cause the output voltage waveform distortion. In this paper, the IFOC method is used to control motor's speed and torque. Thus, a dual loop proportional integral (PI) controller in rotation synchronous frame is applied to control the speed and torque. The controller gains are observed using the pole-zero cancellation method. With capacitor voltage balancing function, the fluctuation of DC-link voltage of is less significant response. This means the DC-link voltage of qZ-source T-type inverter can be stably generated at dynamic load condition. By using TSD PWM, the boost factor of inverter is improved and then and the desired input voltage of the motor drive system is achieved at any change in speed and load. As a result, the efficiency of the motor drive system can also be improved by qZ-source T-type inverter fed vector control using TSD PWM technique.

2. QUASI IMPEDANCE (qZ)-SOURCE T-TYPE INVERTER

Figure 1 illustrates the equivalent circuit of proposed design qZ-source T-type inverter. As seen in Figure 1, there are two impedance networks called upper and lower quasi network. For the symmetrical network, the values of the capacitors, inductors and diodes in the circuit are assumed to be equal so as to easily simplify the network analysis. The upper, v_{C1} and lower capacitor voltages, v_{C3} are equal, $v_{C1} = v_{C3}$. Similarly, the inductor voltages of upper and lower network are equal, $v_{L1} = v_{L3}$. The three main arms of

T-type inverter are composed of the main switches: S_{a1}, S_{a2}, S_{b1}, S_{b2}, S_{c1}, and S_{c2} with freewheeling diodes: D_{a1}, D_{a2}, D_{b1}, D_{b2}, D_{c1}, D_{c2} and three auxiliary arms are composed of the switches, S_{a3}, S_{a4}, S_{b3}, S_{b4}, S_{c3}, and S_{c4} with freewheeling diodes: D_{a3}, D_{a4}, D_{b3}, D_{b4}, D_{c3}, and D_{c4}. To control the upper DC-link capacitor voltage, the upper shoot-through (UST) is applied. The UST can be obtained when the upper shoot-through duty ratio, d_U is applied to the upper switches (S_{x1}, S_{x3}, and S_{x4}). The lower shoot-through (LST) can be obtained when the lower shoot-through duty ratio, d_L is applied to the lower switches (S_{x2}, S_{x3}, and S_{x4}).

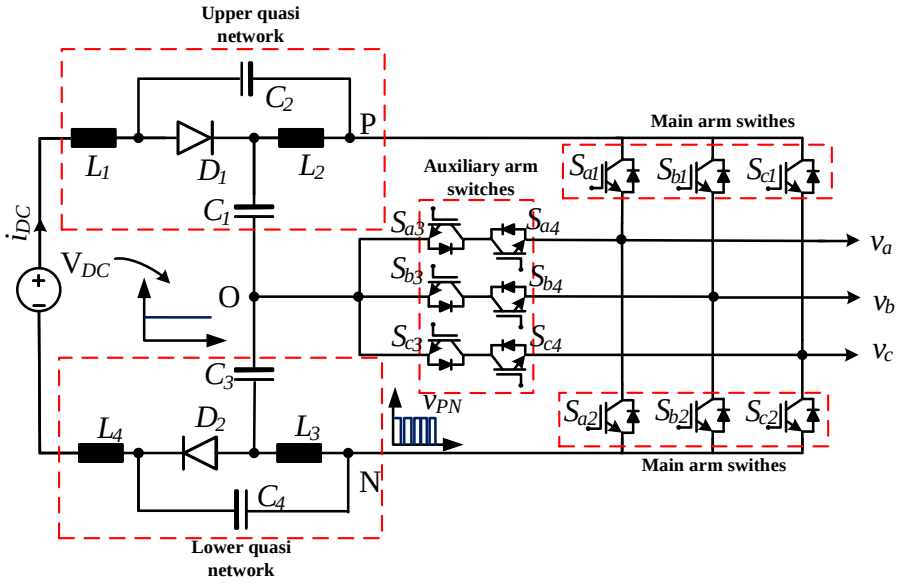

Figure 1. Equivalent circuit of qZ-source T-type inverter

2.1. Switching operations of qZ-source T-type inverter

Table 1 presents the voltage transition output or DC-link voltage and switching states of the qZ-source T-type inverter. Let us considering the one arm operation mode, there are four switches S_{a1}, S_{a2}, S_{a3} and S_{a4}. For the active mode at the positive half period, S_{a1} and S_{a4} are turned ON and S_{a2} and S_{a3} are turned OFF. The positive current is flowing through S_{a1}. Although the switch S_{a4} is turned ON, there is no current flowing through it, and the switch S_{a4} has no conduction loss. For the active mode at the negative half period, S_{a2} and S_{a3} are turned ON and S_{a1} and S_{a4} are turned OFF. The load current is only flowing through S_{a2} but not through S_{a3}. Thus, S_{a3} has no conduction loss in this negative mode.

For the freewheeling mode at the positive half period, the transistor pairs of S_{a3} and S_{a4} are turned ON while S_{a1} and S_{a2} are turned OFF. S_{a4} is always turned ON and has nearly no switching loss in this mode. The load current is flowing through S_{a4} and D_{a1}. For the freewheeling mode at the negative half period, similarly S_{a3} and S_{a4} are ON while Sa_1 and S_{a2} are OFF. In this mode, S_{a3} is always ON and has nearly no switching loss in this mode. Thus, load current is flowing through S_{a3} and D_{a2}.

For upper shoot-through (UST) mode, positive current flow through the S_{a1}, turned ON and then current flow through D_{a4}. Simultaneously S_{a3} is turned ON. For lower shoot-through (LST) mode, load current flow through S_{a2}, turned ON and flow through D_{a3}. Simultaneously, S_{a4} is turned ON. Similarly, arm b and c have the same operation as arm a. According to the switching commutation, the T-type inverter has less switching losses and conduction losses. In this way, UST and LTS can be obtained to control the upper and lower DC-link voltages.

Table 1. Switching State and corresponding output voltage $x \in \{a, b, c\}$

Operation state	Operation switch				Switching output voltage
	$Sx1$	$Sx2$	$Sx3$	$Sx4$	
Positive	1	0	0	1	$\frac{V_{PN}}{2}$
Negative	0	1	1	0	$-\frac{V_{PN}}{2}$
Zero	0	0	1	1	0
Upper shoot-through	1	0	1	0	V_{PO}
Lower shoot-through	0	1	0	1	V_{NO}

2.2. Circuit operation of qZ-source network

The structure is designed by two quasi-impedance (qZ) networks between the DC supply and T-type inverter. There are three sub-circuits operation thus so-called: i) active state, ii) upper shoot-through state, and iii) lower shoot-through state as shown in Figure 2. In qZ-source network, the parasitic resistances of inductor and capacitor, r_L and r_C are considered. The ordinary differential equations from the qZ network operation are described as (1) to (11). Figure 2(a) presents the non-shoot-through or active state. Using Kirchhoff's current law and voltage law, the inductor and capacitor voltages, v_L and v_C and peak DC-link voltage can be obtained as (1) to (3).

$$v_{L1} + v_{L3} = v_{DC} - v_{C1} - v_{C3} - 2i_{L1}(r_L + r_C) \quad (1)$$

$$v_{L2} + v_{L4} = v_{C1} + v_{C3} - 2i_{L2}(r_L + r_C) - i_{PN}r_C \quad (2)$$

$$v_{PN} = v_{PO} + v_{NO} \quad (3)$$

Figure 2(b) depicts the upper shoot-through state. In this state, the upper network is short-circuiting state and lower network is active state. The lower DC-link voltage, v_{NO} can be obtained as (4) to (7).

$$v_{L1} + v_{L3} = v_{DC} + v_{C2} + v_{C4} - v_{NO} \quad (4)$$

$$v_{L2} = v_{C1} \quad (5)$$

$$v_{L4} = v_{C4} \quad (6)$$

$$v_{NO} = v_{C3} + v_{C4} \quad (7)$$

Figure 2(c) illustrates the lower shoot-through state. In this state, the upper network is active state and lower network is shoot-through state. The upper DC-link voltage, v_{PO} can be obtained as (8) to (11).

$$v_{L1} + v_{L3} = V_{DC} + v_{C2} + v_{C4} - v_{PO} \quad (8)$$

$$v_{L2} = -v_{C2} \quad (9)$$

$$v_{L4} = v_{C3} \quad (10)$$

$$v_{PO} = v_{C1} + v_{C2} \quad (11)$$

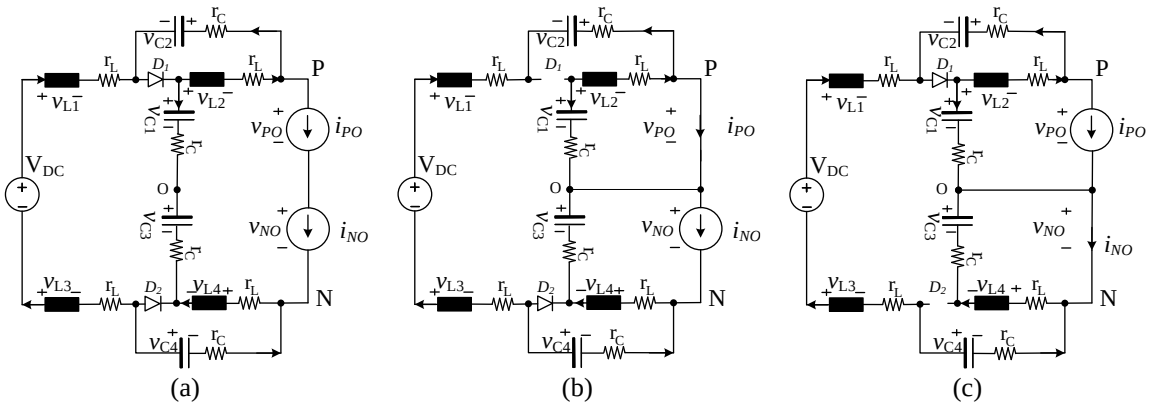

Figure 2. Equivalent circuit for (a) active state, (b) upper shoot-through (UST) state, and (c) lower shoot-through (LST) state

Based on the (1) to (11), the steady-state operating points are represented (12) of quasi network can be derived as in (12):

$$I_{L1} = I_{L2} = I_{L3} = I_{L4} = \frac{1 - D_{STH}}{1 - 2D_{STH}} I_{PN}$$

$$V_{C1} = V_{C3} = \left[\frac{1-D_{STH}}{1-2D_{STH}}\right]\frac{V_{DC}}{2}$$

$$V_{C2} = V_{C4} = \left[\frac{D_{STH}}{1-2D_{STH}}\right]\frac{V_{DC}}{2} \quad (12)$$

The steady-state operating points of upper and lower DC-link voltage, V_{PO} and V_{NO} and output peak phase voltage, $\hat{v}_o$ is derived as (13) to (15).

$$V_{PO} = B_1 \frac{V_{DC}}{2} \quad (13)$$

$$V_{NO} = B_2 \frac{V_{DC}}{2} \quad (14)$$

$$\hat{v}_o = m_a{}^*(B_1 + B_2)V_{DC} \quad (15)$$

where $B_1 = \frac{1}{1-2D_{STH}} \geq 1$ and $B_2 = \frac{1}{1-2D_{STH}} \geq 1$ are the boost factor of upper and lower DC-link voltages, $\hat{v}_o$ is the peak phase output voltage. Modulation index is defined as $m_a{}^*$. The DC-link capacitor voltage V_{PN} can be obtained by adding the upper and lower DC-link voltages (13) and (14).

2.3. PI controller for DC-link capacitor voltages

This work using the small-signal perturbation of state variable form, $\dot{x} = A\tilde{x} + B\tilde{d} + C\tilde{d}$. The control to DC-link capacitor voltage transfer function of the system is given in (16), where D_{STH} is the shoot-through duty ratio of qZ-source impedance T-type inverter.

$$\frac{(\tilde{v}_{C1}+\tilde{v}_{C3})(s)}{\tilde{D}_{STH}(s)} = \frac{4I_{PN}(Ls+2r_C+3r_L-2D_{STH}r_L)-V_{DC}(1-2D_{STH})}{(4CLD_{STH}-2CL)s^2+(4CD_{STH}r_C-2C(r_L+r_C)+4CD_{STH}r_L)s+16D_{STH}^3-24D_{STH}^2+12D_{STH}-2} \quad (16)$$

DC-link voltages are difficult to measure directly due to their discrete nature. Therefore, DC-link voltage can be indirectly measured from the capacitor voltages(v_{C1}, v_{C3}). The capacitor voltage is difficult to control while occurrence of the external disturbance, input fluctuation and its characteristics. PI controller is used to maintain the capacitor voltages to resist the sag and swell the supply side and external disturbances. The network parameters for qZ-source are shown in Table 2.

The plant transfer function is a critical point to find the controller gains (k_p, k_i). The PI controller gain $G_c(s)$ obtains from a comparison of the reference two capacitor voltage ($V^*_{C1}+V^*_{C3}$) and actual two capacitor voltage ($v_{C1}+v_{C3}$). PI controller is to reduce the right-half plane converter effect and eliminate the steady-state error and commonly used in motor drive system. Controller gain generates the shoot-through duty ratio D_{STH} to command the PWM pulse that provides the control pulse for corresponding switch. Figure 3 shows the closed-loop control system of DC-link capacitor voltage.

Table 2. Parameters of qZ-source simulation

Quantity	Symbol	Value	Unit
Input voltage	V_{DC}	300	V
DC-link Voltage	V_{PN}	400	V
Output current	I_{PN}	1	A
Inductors	L_1, L_2, L_3, L_4	0.77	mH
Capacitors	C_1, C_2, C_3, C_4	470	µF
Parasitic resistance	r_L	0.3	Ω
Equivalent resistance	r_C	1.4	Ω

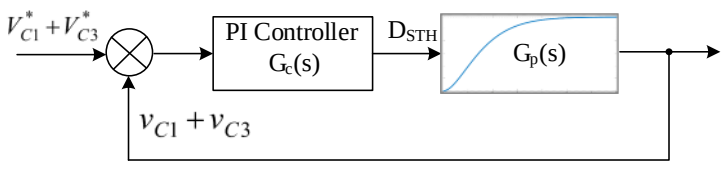

Figure 3. Closed-loop DC-link voltage control structure

The purpose of DC-link voltage control is to regulate the capacitor voltage and utilize the desired voltage. The plant transfer function, $G_p(s)$ of the system is described in (17) which is calculated using parameters shown in Table 2.

$$G_p(s) = \frac{-0.00308s+405.6}{5.067\times10^{-7}s^2+0.001119s+0.686} \quad (17)$$

3. DC-LINK CAPACITOR VOLTAGE-BALANCING FUNCTION WITH TSD PWM METHOD

The pulse width modulation PWM is an essential technique for controlling inverter switching operating mode to achieve a good utilization of output voltage. Traditional boost PWM control methods used in impedance source inverters are simple boost (SB) control, maximum boost (MB) control, maximum constant boost (MCB), and SV control method [19]–[21]. TSD method of the DC-link capacitor voltage and the output voltage are controlled by regulating the modulation index, m_a^*.

3.1. Triple sixty-degree PWM method

The simple boost TSD PWM method is comprehensively based on the dual space vector pulse width modulation (DSVPWM) technique [22]. This SB control method increases the voltage stress and limits the voltage gain due to the switch device voltage rating. Shoot-through duty ratio, D_{STH} is obtained from the DC-link PI control and this ratio should have within the $(1-m_a^*)$. According to the simple boost method, shoot-through limiter, d_{STH} should be less than $(1-m_a^*)$. If under modulation occurred, shoot-through limiter, d_{STH} and shoot-through duty ratio, D_{STH} would become equal due to the MATLAB function algorithm for the capacitor voltage-balancing function.

The TSD PWM method consist of three sets of sixty-degree modulation waves as the reference signals, and medium frequency sawtooth wave, v_{car} represents a carrier signal. Figure 4 presents the triple sixty-degree modulation with one fundamental cycle in which $x \in \{a, b, c\}$. The sixty-degree PWM technique can reduce the harmonic distortion and extend the output magnitude [23]. Sine modulation waves, v_{sinx}^* transformed into sixty-degree modulation 'flat top' wave, v_{SDx}^* using MATLAB function algorithms. The sixty-degree flat top section between 60° and 120° is an upper half cycle and 240° and 300° is a lower half cycle. Modulation index,m_a^* is multiple by 115% toget the input voltage required modulation wave.

The main arm set of sixty-degree modulation reference is v_x^*. The upper set of sixty-degree modulation reference is v_{x2}^*. By adding the sum of upper shoot-through duty ratio, d_U and main arm set, v_{SDx}^* to v_{x2}^*, the lower DC offset is achieved. The lower set of sixty-degree modulation reference is v_{x1}^*. By adding the sum of lower shoot-through duty ratio, d_L and main arm set, v_{SDx}^* to v_{x1}^*, the upper DC offset is achieved. The generated gate signals are shown in Figure 5 with respected to switching operations. The upper and lower shoot-through time, T_{UST} and T_{LST}, upper and lower duty ratio, d_U and d_L. The triple boost factor, B_{TSD} and simple boost factor, B_{SB} can be calculated using (18) to (23). Gate signal generation of sawtooth carrier-based triple sixty-degree modulation waves of half switching cycle for one arm is shown in Figure 5.

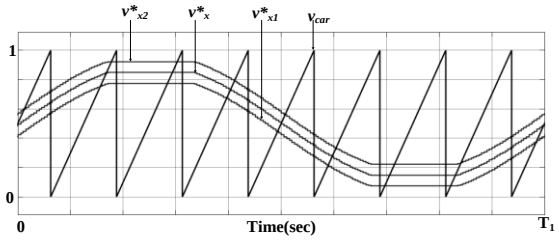

Figure 4. Triple sixty-degree modulation and sawtooth carrier signal for one fundamental cycle

$$d_U = \frac{d_{STH}}{2} \quad (18)$$

$$d_L = \frac{d_{STH}}{2} \quad (19)$$

$$T_{UST} = \text{UpperDCoffset} * \frac{T}{2} \quad (20)$$

$$T_{LST} = \text{LowerDCoffset} * \frac{T}{2} \quad (21)$$

$$B_{TSD} = \frac{1}{3m_a^* - 2} \quad (22)$$

$$B_{SB} = \frac{1}{2m_a^* - 1} \quad (23)$$

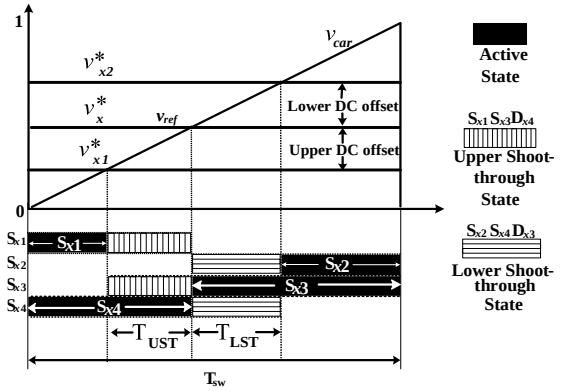

Figure 5. Generating TSD PWM for operating region in half fundamental cycle of T-type inverter

3.2. DC-link capacitor voltage-balancing control method

The important point of DC-link voltage control is balancing the two capacitor voltages v_{C1} and v_{C3}. Without matching the two capacitor voltages, DC-link voltage cannot regulate and it affects the output voltage that may lead to achieve the poor performance with the drive system. Therefore, it is required to use the correct value of gain and remove the steady-state error. The same upper and lower duty ratio, $d_U = d_L$ can be achieved by balancing two capacitor voltages from shoot-through limiter, d_{STH}. When the upper capacitor voltage, v_{C1} is less value than the lower capacitor voltage, v_{C3} the balancing value, Δd is added to upper shoot-through limiter ($d_U = d_{STH} + \Delta d$) to be balanced as the lower capacitor voltage. When the lower capacitor voltage, v_{C3} is less value than the upper capacitor voltage, v_{C1} the balancing value, Δd is added to lower shoot-through limiter ($d_L = d_{STH} + \Delta d$) to be balanced as the upper capacitor voltage. Balancing value should be carefully chosen because this may occur the over-boost and lead to damage the passive component value of quasi network. Overall system block and MATLAB function block of the system are explained in following section.

3.3. Software implementation of qZ-source T-type inverter fed induction motor drive system

This section explains the software implementation of qZ-source T-type inverter with IFOC based induction motor drive system used the TSD PWM method. The field-oriented control is very popular in industrial motor drive system because this technique based on the control of both magnitude and direction of motor current and furthermore, it can control the dynamic condition of motor drive system. The overall block diagram is illustrated in Figure 6. Single-phase 220 V, 50 Hz AC supply is transformed into 300 V DC supply to qZ-source T-type inverter is applied to a three-phase induction motor.

For IFOC based speed and current control, the line current, i_{abc} is transformed into a rotating synchronous reference frame current, i^e_{dqs} by using the direct Park transformation to reduce the complexity of the differential equations. λ^{e*}_{dr} and T^*_e are defined as the reference amplitude of the rotor flux and electromagnetic torque. The speed error is the difference between the reference speed, ω^*_m and the estimated speed, ω_m. The output of the PI speed controller is the reference torque, T^*_e. The reference d-axis stator current, i^{e*}_{ds} controls the rotor flux, λ^{e*}_{dr}, whereas the reference q-axis stator current, i^{e*}_{qs} also controls the torque, T^*_e. The current error is the difference between the reference dq current, i^{e*}_{dqs} and dq current, i^e_{dqs} applied to the PI controllers. Rotor angle, θ_e is obtained from the slip angular frequency, ω_{sl}. The current controller output, v^{e*}_{dq} is multiplied by half DC-link capacitor voltage, $\frac{2}{v_{PN}}$ to achieve the modulation index of $m_{dq}{}^*$. System component values are synchronous reference frame denote as superscript 'e'. The PI controller accomplished the DC-link voltage, speed, and current of the motor drive system by using the feedback control. The magnitude modulation vector, m^*_a is defined in (24) which is injected into the TSD modulation block and shoot-through limiter block.

$$m_a^* = \sqrt{(m_d{}^*)^2 + (m_q{}^*)^2} \quad (24)$$

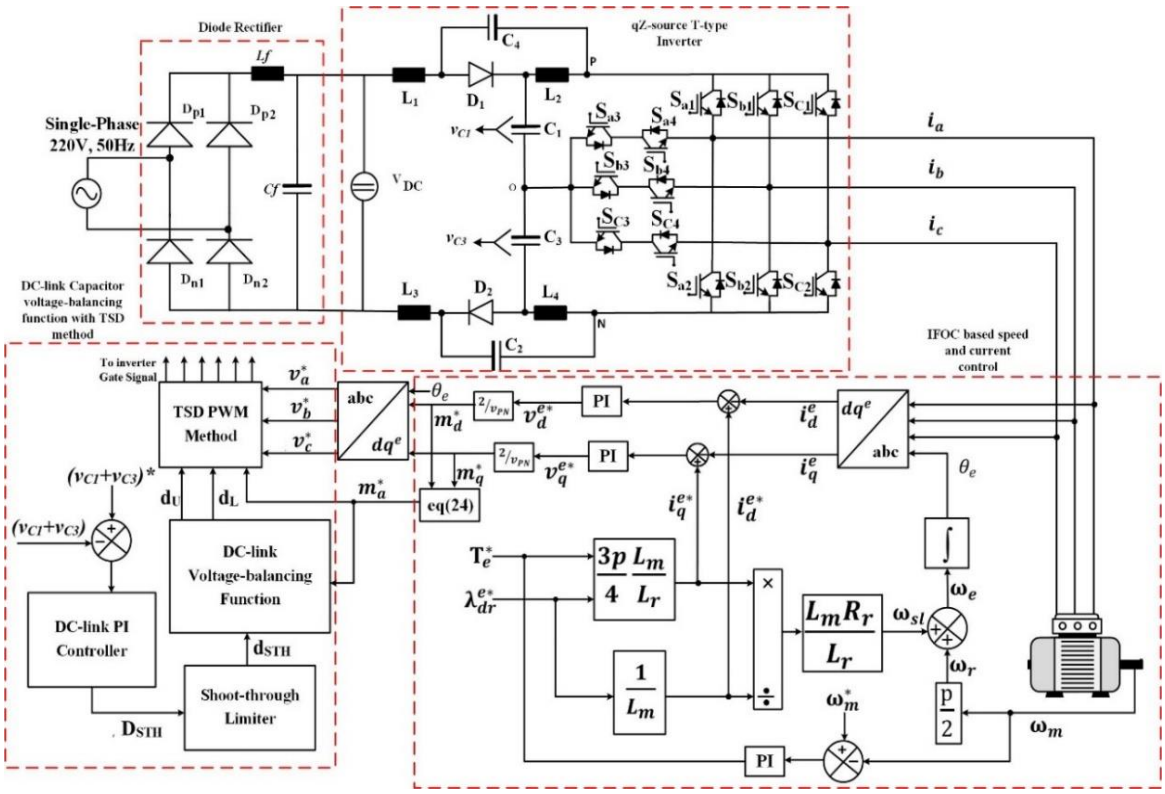

Figure 6. Block diagram for induction motor drive system

IFOC strategy and the induction motor model are expressed in [24], [25]. Feed-forward components are out of scope for this current controller design. The IFOC based dual-loop speed and current PI controller gains are achieved by using the pole-zero cancellation method to improve the induction motor dynamic response. The pole-zero cancellation method was used to select the speed and current controller gains as guided [26] and PI gain values and bandwidth frequency are described in Table 3.

Table 3. Current and speed PI controller gains

PI controller gain	Current control		Speed control	
	k_{pc}	k_{ic}	k_{pm}	k_{im}
	28.8687	6.811×10^4	9.5532	2.1768
Bandwidth frequency(rad/sec)	$2.513\times10^3(\omega_{ci})$		$251.3274(\omega_{cm})$	

3.4. Workflow configuration for gate signal generation

For induction motor drive system, the indirect FOC method is used to control the dynamic performance of the motor. Figure 7 illustrated the workflow process of this system. From the IFOC of speed and current motor drive PI control, getting the modulation index, m_a^* and rotating angle, θ_e. These are injected into the reference sine wave, which is transformed into sixty-degree modulation using the MATLAB function algorithm. Control to DC-link capacitor voltage ration (16) generates the shoot-through duty ratio, D_{STH} to provide the PWM pulse. Due to the simple boost limitation, to control the upper and lower DC-link capacitor voltage v_{c1} and v_{c3}, D_{STH} is transformed into upper and lower duty ratio d_U and d_L using the MATLAB function algorithm. These two-duty ratio are applied to the TSD PWM block which generates the three sixty-degree reference waves. Finally, three reference waves and sawtooth carrier wave are compared and then achieve the active, upper and lower shoot-through gate pulse. TSD PWM method has more boost factor than simple boost PWM method because of (22) and (23) and explained in the next section.

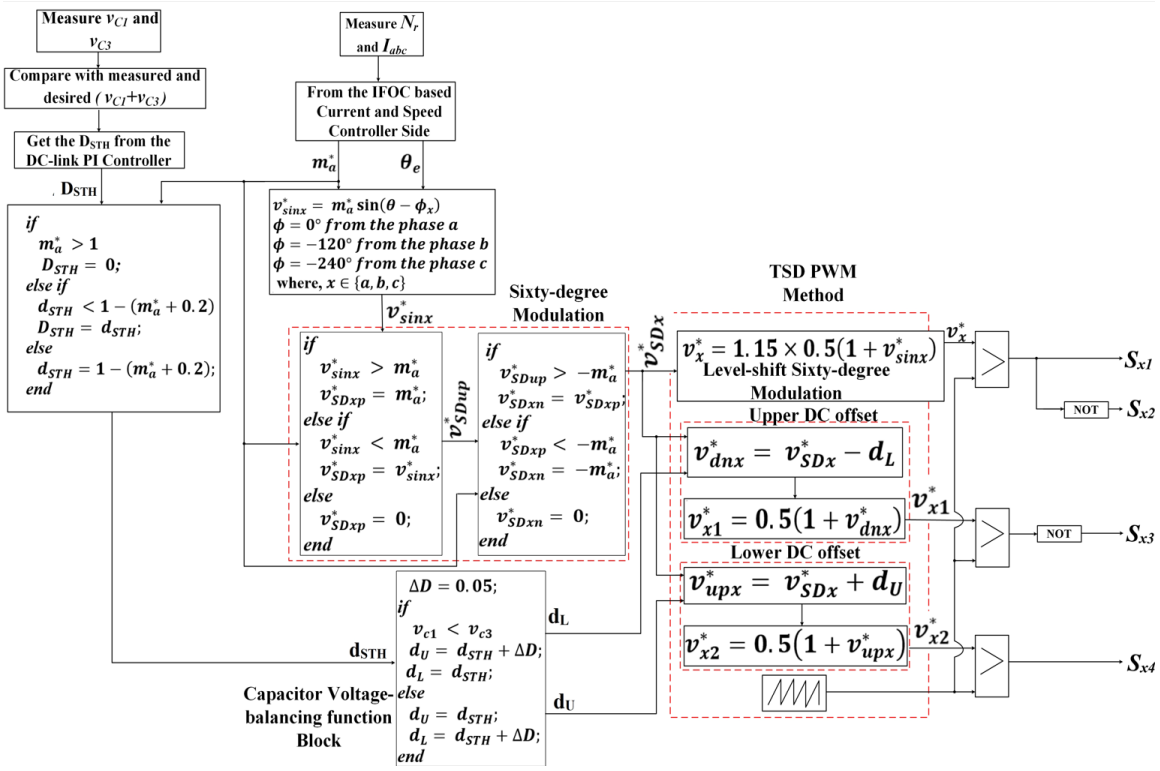

Figure 7. Workflow configuration for gate signal generation

4. RESULTS AND DISCUSSION

Simulation work was carried out by using MATLAB/Simulink software. The frequency responses at various PI gains of DC-link capacitor voltage controller were firstly observed. From the results, the PI gains, phase and gain margin were selected for the next step simulation.

4.1. Frequency response of DC-link capacitor voltages PI controller

To control the DC-link capacitor voltages (v_{c1} and v_{c3}), the PI controller was used. In this study, the PI gains (k_p and k_i) are set from 0.01 to 0.1 for k_p and 10 for k_i. The frequency responses of DC-link capacitor voltage PI controller are shown in Figure 8(a) step response Figure 8(b) bode plot. As seen in Figure 8(a), the response while k_{p3}=0.1 and k_{i3}=10 has faster response, settling time is 0.006 sec and zero steady-state error. To maintain stability under variations in circuit characteristics caused during operation, the phase and gain margin are calculated at different k_p and k_i values. The according to the results, bandwidth crossover frequency (CF_3) 1.9×10^4 rad/sec is at phase margin PM_3=17.2°, gain margin GM_3=19 dB. This means the system is stable at k_{p3}=0.1, k_{i3}=10. Therefore, this can be a well-tried DC-link capacitor voltage PI control for this work.

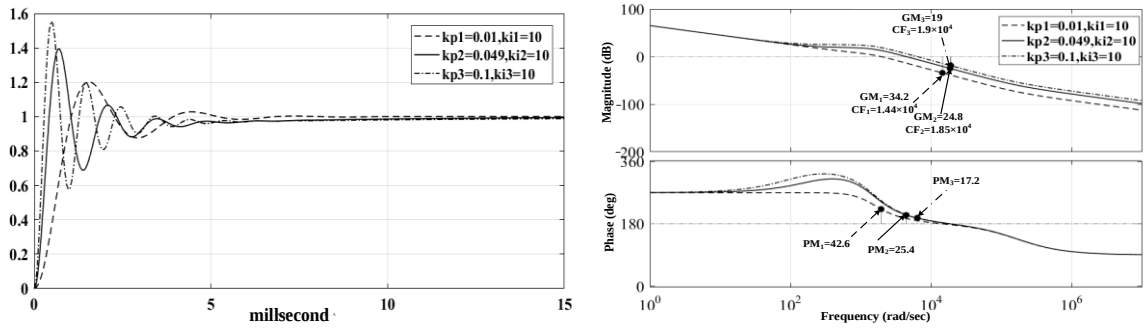

Figure 8. Corresponding simulated result for step response and frequency response for, (a) response of the DC-link capacitor voltage with PI controller and (b) bode plot for frequency response with PI controller

4.2. Comparisons between simple boost sixty-degree and triple sixty-degree PWM method

The modulation index, m_a^* of the triple sixty-degree PWM method was calculated to get the upper and lower duty ratios (d_U and d_L). In this work, the comparisons between m_a^* of the simple boost sixty-degree (SBSD) and TSD PWM method were done. The modulation index,m_a^* using both methods are shown in Figures 9(a) and (b) with respect to the boost factors and output peak phase voltage of the inverter. Using TSD PWM method, the boost factor can be improved twice at $m_a^* = 0.75$ of that using SBSD. However, when m_a^* is closed to 1, the factors using both methods are decreased. According to the (22) and (23), the boost factors are inversely proportional to the modulation index, m_a^*. Moreover, m_a^* should be less than 1. For this work, boost factor (1.18) and m_a^* (0.95) are chosen in considering of motor rating. SBSD method cannot achieve the required line voltage at this point. According to the (18) and (19), d_U and d_L can be calculated from the shoot through limiter, d_{STH} where d_{STH} is (1- m_a^*). Using (15), the output peak phase voltage,$\hat{v}_o$ can be calculated as shown in Figure 9(b). The phase voltages are increased when the modulation index is decreased. Using TSD PWM method, the higher output voltage can be achieved comparing with SBSD at the same modulation index. Therefore, TSD PWM method could be used for motor drive system which consumes higher voltage rating.

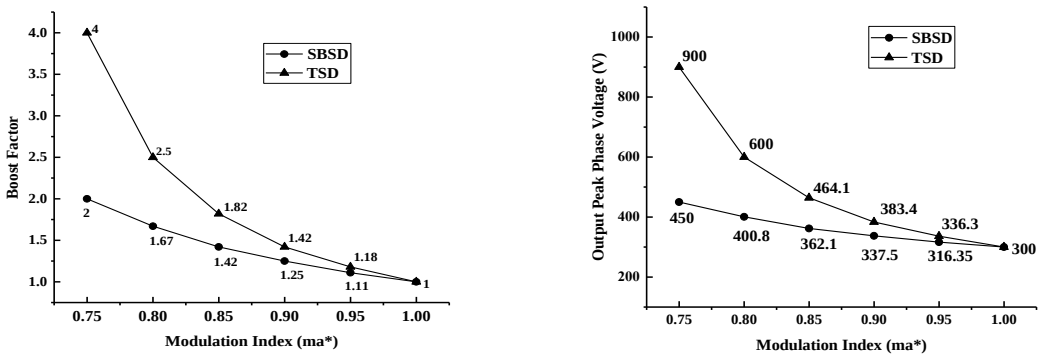

(a) (b)

Figure 9. Relationship between modulation index with (a) boost factor and (b) output phase voltage

4.3. With and without balancing control of the qZ-source T-type inverter fed induction motor drive

The characteristics of dq-axes current, i_{dqs}^e, load torque, T_e and rotating speed, N_r for drive system were studied with and without the DC-link capacitor voltage-balancing function. In order to study the dynamic state of motor drive system with and without DC-link capacitor voltage-balancing function, the simulation has been carried out for the cases: i) DC supply change, ii) speed change and iii) torque change. Table 4 represents the parameters of three-phase induction motor proposed to be used in this work. The reference DC-link capacitor voltage (V_{C1}+V_{C3})* is set as 400 V and the operating time is 8 sec and m_a^*=0.95, d_U and d_L=0.05 and switching frequency, f_{sw}=8 kHz are set for software implementation.

Table 4. Induction motor parameters used for simulation

Description	Symbol	Value	Unit
Power rating	P	4	kW
Line to line (rms)	V_{LL}	400	V
Line frequency	f	50	Hz
Rotor Rated Speed	N_r	1400	rpm
Stator Resistance	R_s	1.405	Ω
Stator Inductance	L_s	0.005839	H
Rotor resistance	R_r	1.395	Ω
Rotor Inductance	L_r	0.005839	H
Mutual Inductance	L_m	0.1722	H
Moment of Inertia	J	0.0131	Kg-m^2
Friction factor	B	0.002985	-
Pole Pair	P	2	-

4.3.1. Case 1: disturbance of DC supply voltage

Under this condition, the DC supply voltage (300 V) is applied to qZ-source T-type inverter while the motor is operating at constant speed 1400 rpm and load torque 1 N-m. After 3 sec, the applied DC voltage

changes to 250 V as seen in Figure 10. After 6 sec, it arises back to 300 V. In this case, changes in DC supply voltage because of the input fluctuation are considered.

Figure 11 shows the response of the qZ-source T-type Inverter fed Induction motor drive with DC Supply Disturbance. According to the simulation result without capacitor balancing function as shown in Figure 11(a), DC-link capacitor voltages are significantly mismatched during operation. With capacitor balancing function, there is no significant change in DC-link capacitor voltage, Figure 11(b).

4.3.2. Case 2: changes in reference speed step of the motor

In order to operate motor drive system with 1,400 rpm reference speed, the motor is started to operate with 700 rpm and then stepped to1,400 rpm at 4 sec as seen in Figure 12. The DC supply voltage 300 V and load torque 1 N-m are remained constant. As a result, the actual speed response follows the reference speed with few milliseconds of delay to reach the desired speed. Figure 13 shows the characteristics DC-link capacitor voltages while setting to rated speed with and without capacitor balancing function. Without balancing function, when the motor is not operating at rated speed with 1,400 rpm, there is mismatching between the two capacitor voltages as seen Figure 13(a). Even though the speed step changes to rated speed, the capacitor voltages are still not equally operating and it may take some times to operate equally. With balancing function, DC-link capacitor voltage occurs significantly overshot at rated speed increased as shown Figure 13(b). Figures 14 and 15 show the rotating dq-axes current at reference speed step-change. Both rotating d-axis current for without balancing control in Figure 14(a) and with balancing control in Figure 14(b) have a high flux density in speed change of the motor at 4-sec. Both rotating q-axis current for without balancing control in Figure 15(a) and with balancing control in Figure 15(b) occurred sharp rise of current at 4 sec.

4.3.3. Case 3: changes in load torque

In this case, the torque is increased from no-load to 2 N-m loads at a constant supply voltage of 300 V and a constant speed of 1,400 rpm. According to the simulation result, the actual response of load torque follows the reference load change as shown in Figure 16. Without balancing function, the DC-link capacitor voltages are fluctuated at initial t= 0-2 sec, then the DC-link capacitor voltages are not stable the desired voltage 200 V from no-load to load. With balancing function, the DC-link capacitor voltages are stable from no-load to load, except the initial fluctuation for 0.15 sec expressed in Figure 17(a). This means adopting the capacitor balancing function to the qZ-source T-type inverter can control the DC-link capacitor voltages during the transition of no-load to load condition of the motor as shown in Figure 17(b).

Speed and torque results were possible to verify the response of the PI controller. Without using the capacitor voltage-balancing function, DC-link each capacitor value does not have the 200 V. Using the capacitor voltage-balancing condition, each DC-link capacitor voltage achieves the desired voltage of 200 V. In case 2 with voltage-balancing function, when the rated speed step changed, that also slip changes, but the motor runs at rated torque and constant DC supply; therefore, the DC-link voltage significant fluctuation occurs at speed increased point.

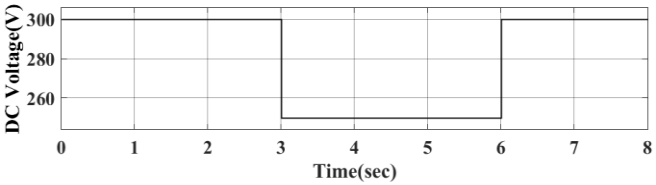

Figure 10. DC supply voltage step change

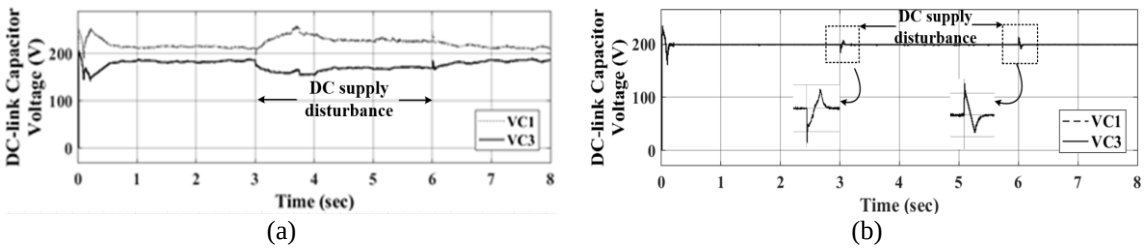

Figure 11. Comparing the software results in dc-link capacitor voltage at dc supply disturbance (a) without balancing function and (b) with balancing function

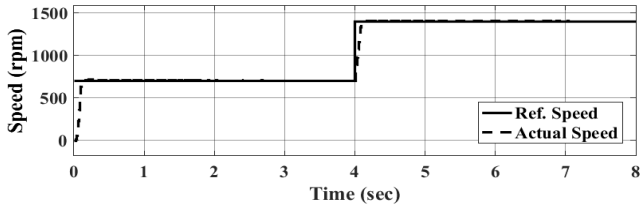

Figure 12. Speed step change response of the motor drive system

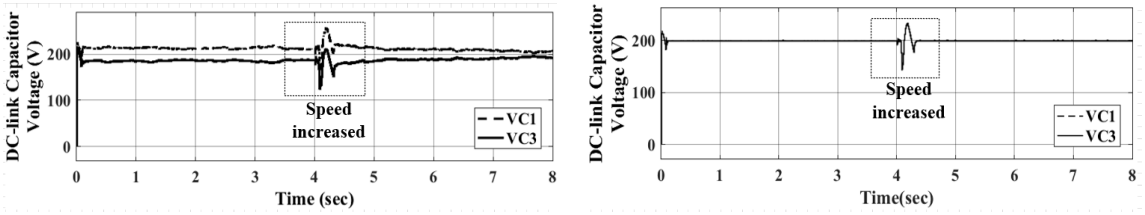

Figure 13. Speed step change response of the motor drive system with DC-link capacitor voltage at (a) without balancing function and (b) with balancing function

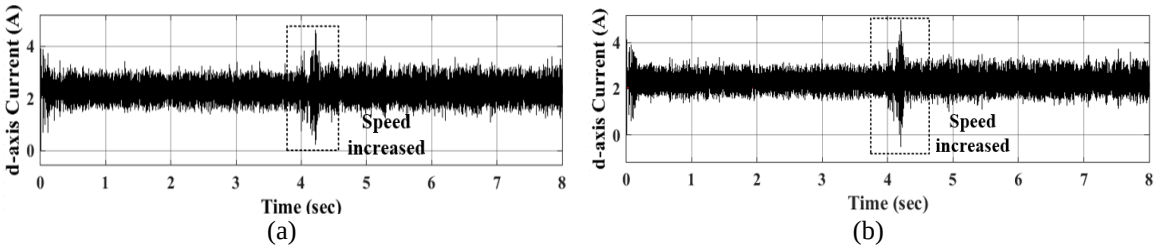

Figure 14. Speed step change response of the motor drive system with rotating d-axis current at (a) without balancing function and (b) with balancing function

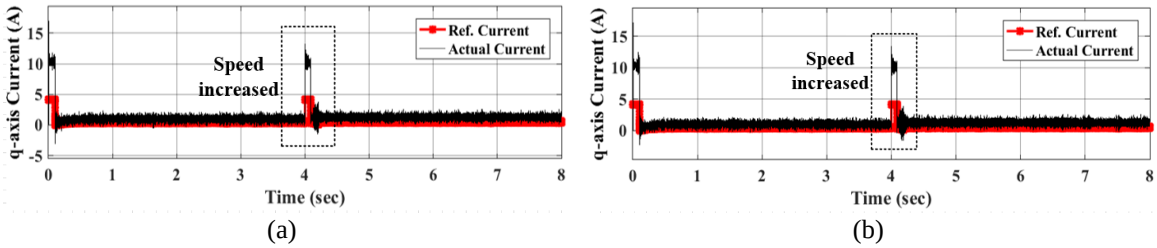

Figure 15. Speed step change response of the motor drive system with rotating q-axis current at (a) without balancing function and (b) with balancing function

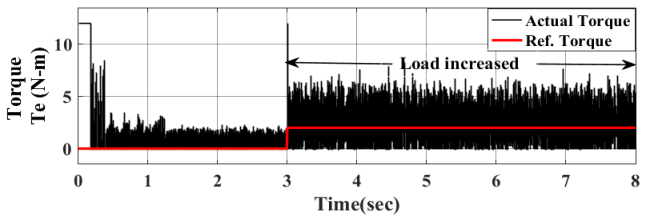

Figure 16. Load torque change response of the motor drive system

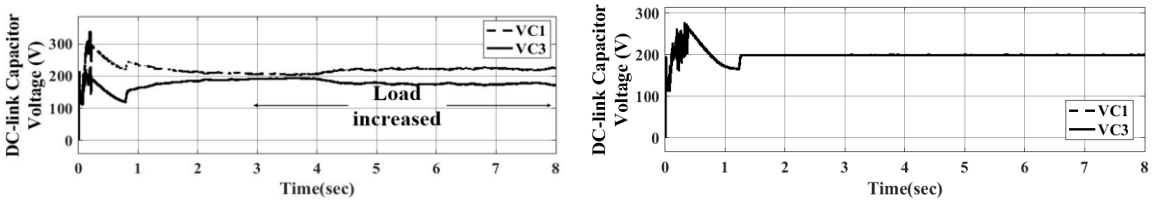

Figure 17. Load torque change response of the motor drive system with DC-link capacitor voltage at (a) without balancing function and (b) with balancing function

5. CONCLUSION

This paper presents DC-link voltage control of the qZ-source T-type inverter fed IFOC based induction motor drive system with the simple boost triple sixty-degree PWM method. The capacitor voltage-balancing function with the TSD technique can achieve significant equal voltage sharing on two DC-link capacitor voltages of the inverter. By comparing with/without using capacitor balancing function, qZ-source T-type inverter of TSD PWM with capacitor voltage balancing function could provide DC-link capacitor voltages equally. The simulation model of TSD PWM method generates more extended output peak phase voltage with 336 V than SBSD method (316 V). Thus, the line voltage of the motor is 400 V. The performance results are robust and continue to track the reference value by adequately designing the current and speed PI controller gains. According to the simulation results, the drive system has effective speed and current control, and the capacitor voltage-balancing function achieves satisfactory results. Therefore, the system has high reliability. According to the simulation results, the RMS voltage of the motor is 408 V and the current is 8.5 A, and then the power consumption of the motor can be calculated as 4.13 kW. The system achieved the fast response and less steady-state error by using PI controller for the DC-link voltage controller. Thus, this motor drive system with qZ-source T-type inverter using TSD PWM method could be used for rolling mill. In the near future, a small-scale experiment test will be carried out to validate the simulation result of qZ-source T-type inverter fed induction motor drive system. Therefore, a triple sixty-degree sawtooth carrier-based with capacitor voltage-balancing function is suitable for this drive system.

REFERENCES

[1] F. Z. Peng, "Z-source inverter," *IEEE Transactions on Industry Applications*, vol. 39, no. 2, pp. 504–510, Mar. 2003, doi: 10.1109/TIA.2003.808920.
[2] R. M. Strzelecki and D. Vinnikov, "Models of the qZ-Converters," *Przeglad Elektrotechniczny*, vol. 86, no. 6, pp. 80–84, 2010.
[3] F. Z. Peng *et al.*, "Z-source inverter for motor drives," *IEEE Transactions on Power Electronics*, vol. 20, no. 4, pp. 857–863, Jul. 2005, doi: 10.1109/TPEL.2005.850938.
[4] M. K. Islam, M. M. Zaved, A. M. Siddiky, and K. A. Al Mamun, "A comparative analysis among PWM control Z-source inverter with conventional PWM Inverter for induction motor drive," in *2016 International Conference on Innovations in Science, Engineering and Technology (ICISET)*, Oct. 2016, pp. 1–6, doi: 10.1109/ICISET.2016.7856496.
[5] L. Ping, L. He-ping, and H. Jian-ye, "Transient analysis of DC-link voltage for Z-source converter considering parasitic parameters," *Procedia Engineering*, vol. 15, pp. 230–234, 2011, doi: 10.1016/j.proeng.2011.08.046.
[6] E. Makovenko, O. Husev, J. Zakis, C. Roncero-Clemente, E. Romero-Cadaval, and D. Vinnikov, "Passive power decoupling approach for three-level single-phase impedance Source Inverter based on resonant and PID controllers," in *2017 11th IEEE International Conference on Compatibility, Power Electronics and Power Engineering (CPE-POWERENG)*, 2017, pp. 516–521, doi: 10.1109/CPE.2017.7915225.
[7] Y. Liu, B. Ge, F. J. T. E. Ferreira, A. T. de Almeida, and H. Abu-Rub, "Modeling and SVPWM control of quasi-Z-source inverter," in *11th International Conference on Electrical Power Quality and Utilisation*, 2011, pp. 1–7, doi: 10.1109/EPQU.2011.6128914.
[8] I. A. Bakhovtsev and D. V. Panflov, "Three-phase three-level voltage source inverter construction based on quasi-Z-source cells," in *2013 14th International Conference of Young Specialists on Micro/Nanotechnologies and Electron Devices*, Jul. 2013, pp. 322–327, doi: 10.1109/EDM.2013.6642005.
[9] D. Panfilov, O. Husev, F. Blaabjerg, J. Zakis, and K. Khandakji, "Comparison of three-phase three-level voltage source inverter with intermediate dc–dc boost converter and quasi-Z-source inverter," *IET Power Electronics*, vol. 9, no. 6, pp. 1238–1248, May 2016, doi: 10.1049/iet-pel.2015.0539.
[10] F. Barrero-González *et al.*, "Improvements on the carrier-based control method for a three-level T-type, quasi-impedance-source inverter," *Electronics*, vol. 8, no. 6, Jun. 2019, doi: 10.3390/electronics8060677.
[11] M. Schweizer and J. W. Kolar, "High efficiency drive system with 3-level T-type inverter," in *Proceedings of the 2011 14th European Conference on Power Electronics and Applications*, 2011, pp. 1–10.
[12] S.-M. Shin, J.-H. Ahn, and B.-K. Lee, "Maximum efficiency operation of three-level T-type inverter for low-voltage and low-power home appliances," *Journal of Electrical Engineering and Technology*, vol. 10, no. 2, pp. 586–594, Mar. 2015, doi: 10.5370/JEET.2015.10.2.586.
[13] A. Tuluhong, W. Wang, Y. Li, and L. Xu, "A novel hybrid T-type three-level inverter based on SVPWM for PV application," *Journal of Electrical and Computer Engineering*, vol. 2018, pp. 1–12, Jun. 2018, doi: 10.1155/2018/7245039.
[14] A. Zorig, M. Belkheiri, and S. Barkat, "Control of three-level T-type inverter based grid connected PV system," in *2016 13th International Multi-Conference on Systems, Signals & Devices (SSD)*, Mar. 2016, pp. 66–71, doi: 10.1109/SSD.2016.7473723.

[15] D. C. Happyanto, A. W. Aditya, and B. Sumantri, "Boundary–layer effect in robust sliding mode control for indirect field oriented control of 3-phase induction motor," *International Journal on Electrical Engineering and Informatics*, vol. 12, no. 2, pp. 188–204, Jun. 2020, doi: 10.15676/ijeei.2020.12.2.2.
[16] Y. Wang, Y. Shi, Y. Xu, and R. D. Lorenz, "A comparative overview of indirect field oriented control (IFOC) and deadbeat-direct torque and flux control (DB-DTFC) for AC Motor Drives," *Chinese Journal of Electrical Engineering*, vol. 1, no. 1, pp. 9–20, Dec. 2015, doi: 10.23919/CJEE.2015.7933134.
[17] A. Yousef and S. A. Maksoud, "Review on field oriented control of induction motor," *International Journal for Research in Emerging Science and Technology*, vol. 2, no. 7, pp. 5–16, 2015.
[18] R. Gouws, "Efficiency analysis of an induction motor with direct torque and flux control at a hot rolling mill," in *2011 Proceedings of the 8th Conference on the Industrial and Commercial Use of Energy*, 2011, pp. 64–68.
[19] O. Ellabban, J. Van Mierlo, and P. Lataire, "Capacitor voltage control techniques of the Z-source inverter: A comparative study," *EPE Journal*, vol. 21, no. 4, pp. 13–24, Dec. 2011, doi: 10.1080/09398368.2011.11463806.
[20] B. Y. Husodo, M. Anwari, S. M. Ayob, and Taufik, "Analysis and simulations of Z-source inverter control methods," in *2010 Conference Proceedings IPEC*, Oct. 2010, pp. 699–704, doi: 10.1109/IPECON.2010.5697016.
[21] M. S. Bakar, N. A. Rahim, K. H. Ghazali, and A. H. M. Hanafi, "Z-source inverter pulse width modulation: A survey," in *International Conference on Electrical, Control and Computer Engineering (InECCE)*, 2011, pp. 313–316, doi: 10.1109/INECCE.2011.5953898.
[22] A. K. Akkarapaka and D. Singh, "An IFOC-DSVPWM based DC-Link voltage compensation of Z-source inverter fed induction motor drive for EVs," *Advances in Power Electronics*, vol. 2015, pp. 1–14, Aug. 2015, doi: 10.1155/2015/185381.
[23] A. Rahman, M. M. Rahman, and M. R. Islam, "Performance analysis of three phase inverters with different types of PWM techniques," in *2017 2nd International Conference on Electrical & Electronic Engineering (ICEEE)*, Dec. 2017, pp. 1–4, doi: 10.1109/CEEE.2017.8412864.
[24] I. Ferdiansyah, M. R. Rusli, B. Praharsena, H. Toar, Ridwan, and E. Purwanto, "Speed control of three phase induction motor using indirect field oriented control based on real-time control system," in *2018 10th International Conference on Information Technology and Electrical Engineering (ICITEE)*, Jul. 2018, pp. 438–442, doi: 10.1109/ICITEED.2018.8534864.
[25] K. Zeb, Z. Ali, K. Saleem, W. Uddin, M. A. Javed, and N. Christofides, "Indirect field-oriented control of induction motor drive based on adaptive fuzzy logic controller," *Electrical Engineering*, vol. 99, no. 3, pp. 803–815, Sep. 2017, doi: 10.1007/s00202-016-0447-5.
[26] S. H. You, K. Bonn, D. S. Kim, and S.-K. Kim, "Cascade-type pole-zero cancellation output voltage regulator for DC/DC boost converters," *Energies*, vol. 14, no. 13, pp. 3824–3838, Jun. 2021, doi: 10.3390/en14133824.

BIOGRAPHIES OF AUTHORS

Thin Zar received her Bachelor of Engineering (Electrical Power) degree from Technological University, Meiktila, Myanmar, in 2009, and a Master of Engineering (Electrical Power) degree from Mandalay Technological University, Myanmar, in 2017. She is a lecturer from the Department of Electrical Power Engineering at Government of Technical Institute, Hakha, in Chin State, Myanmar. At present, she is a Ph.D. candidate from the Department of Electrical Power Engineering, Mandalay Technological University, Myanmar. Her research focuses on Quasi Impedance Source T-type Inverter and a power converter for the motor drive and motor control. She can be contacted at lotusthinzar.mdy@gmail.com.

Mai Kai Suan Tial received her B.E. and M.E. degree from the Department of Electrical Power Engineering, Technological University, Myanmar in 2006 and 2009 respectively. From 2010 to 2014, she was working as assistant lecturer at Department of Electrical Power Engineering, Yangon Technological University, Yangon, Myanmar. She received her Ph.D. degree in Electrical Engineering from the Graduate School of Engineering of Kanazawa University, Kanazawa, Japan, in 2017. From 2017 to 2018, she continued to work as an assistant lecturer at Yangon Technological University, and then she was working as lecturer at Department of Electrical Power Engineering, Mandalay Technological University, Mandalay, Myanmar until 2019. She is currently working at Yangon Technological University. Her research interests are power control and development of plasma source and its applications for agricultural soil treatment, waste water treatment and environmental issues. She can be contacted at maikaisuantial21@gmail.com.

Tun Lin Naing received his Bachelor of Engineering (Electrical Power) degree from Mandalay Technological University, Myanmar, and Master of Engineering (Electrical Power) degree from Yangon Technological University, Myanmar, in 2003 and 2006, respectively, and the Ph. D. degree in Electrical Power Engineering from Mandalay Technological University, Myanmar, in 2008. He is a full-time Professor in the Department of Electrical Power Engineering at Mandalay Technological University, Myanmar. His research focuses on mathematical modeling, simulation, and control of power electronic converters. He can be contacted at tunlinnaing1980@gmail.com.